

Response to Reviewer #1 Minor Revisions

Suggestions for revision or reasons for rejection (will be published if the paper is accepted for final publication)

I feel that the authors response and additional analysis do a good job of addressing my initial concerns. I would recommend this work for publication after the consideration of a few very minor further comments.

- The new discussion of the MOC with respect to my second question is useful. I have two further suggestions:

- It would be good to see the absolute numbers relating to the AMOC strength change showing in figure S5 (assuming this is what was referred to as figure S6?), that way the reader could decide whether this is likely to be important within the results.

Thank you for this suggestion, we have added the total AMOC values as a separate panel in figure S5.

- My previous point regarding the MOC contribution was presumably not very clear. I will try to explain this better here. Most people would suggest that the AMO and AMOC are closely related, so if the model is not capturing AMOC variability that co-varies with the AMO signal, they may question whether the model is missing an important component of change driven by AMOC variability - a suggestion I believe previously put forward by the co-author. It would be good for the discussion to tackle this point specifically. This could be done with a minimal reworking on the paragraph starting on line 6 of page 10.

Thank you for raising this point. We do mention the possibility of an AMO/AMOC connection, but there is a lag between the circulation change (AMOC) and the SST response (AMO). Stronger overturning and AMOC over time may manifest itself as positive SST anomalies and thus positive AMO, but this takes time. Latif et al. 2004 show oceanic heat transport through the MOC as leading the SST response by about 10 years, while Delworth and Mann (2000) discuss a 10-year lag between subsurface temperature anomalies and MOC.

While there are many modeling and paleoclimate reconstruction studies proposing a link between AMOC and AMO, the short instrumental record and limited spatial extent of AMOC observations limits our ability to test this hypothesis (Kavvada et al., 2013 and references therein; Delworth and Mann, 2000).

Furthermore, we mention a study by Booth et al. (2012) who showed that the AMO may in fact be explained by variations in aerosol transport and thus not related to AMOC as others suggest.

It is true that the model does not represent an un-verified, only postulated, AMO / AMOC relationship. However, given that this relationship is not supported by data and there are entirely alternative mechanisms with some evidence in support, the model cannot be said to be missing something that is clearly important to the circulation.

We have included additional discussion to this part of the manuscript.

- The statement 'The physical model was spun up for 100 years' needs more detail - how was it spun up? It would be useful to have a little more detail here.

Thank you for this question. For model spin up, the observed meteorological forcing for 1948-1978 was cycled three times (90 years), and then 1948 was repeated 10 years prior to beginning the simulation analyzed here. We will add this detail to the text.

- The manuscript could benefit from further proof reading - e.g. Page 2, line 24

Yes, certainly! Thank you for pointing this out.

References used in Response:

Booth, B. B. B., N. J. Dunstone, P. R. Halloran, T. Andrews, N. Bellouin (2012), Aerosols implicated as a prime driver of twentieth-century North Atlantic climate variability. *Nature*, **484**, 228-232, doi:10.1038/nature10946.

Delworth, T. L., and M. E. Mann (2000), Observed and simulated multidecadal variability in the Northern Hemisphere, *Clim. Dyn.*, 16, 661–676, doi:10.1007/s003820000075.

Kavvada, A. A. Ruiz-Barradas and S. Nigam (2013), AMO's structure and climate footprint in observations and IPCC AR5 climate simulations, *Climate Dynamics*, **41-5**, 1345-1364.

Latif, M., E. Roeckner, B. Botzet, M. Esch, H. Haak, S. Hagemann, J. Jungclauss, S. Legutke, S. Marsland, and U. Mikolajewicz (2004), Reconstructing, Monitoring, and Predicting Multidecadal-Scale Changes in the North Atlantic Thermohaline Circulation with Sea Surface Temperature, *J. Climate*, 17:7, 1605-1614.

DOI: [http://dx.doi.org/10.1175/1520-0442\(2004\)017<1605:RMAPMC>2.0.CO;2](http://dx.doi.org/10.1175/1520-0442(2004)017<1605:RMAPMC>2.0.CO;2).

List of Changes to Manuscript and Supplementary:

1. Additional AMO/AMOC discussion (lines 10-15 on page 10)
2. Spinup model detail added, lines 3-5 page 4
3. Addition of total MOC time series to Supplementary

figure S5

4. Moved Figure 7 to Figure 5 to be consistent with order mentioned in text, and additional proofreading

1 Climate impacts on multidecadal pCO₂ variability in the North 2 Atlantic: 1948-2009

3
4 **Melissa L. Breeden*** and **Galen A. McKinley**

5 Department of Atmospheric and Oceanic Sciences, University of Wisconsin, Madison,
6 Wisconsin, USA

7 *Corresponding author: mbreeden@wisc.edu; 1225 W. Dayton St. Madison, WI 53706
8

9 **Abstract**

10 The North Atlantic is the most intense region of ocean CO₂ uptake in term of units per area.

11 | Here, we investigate multidecadal timescale variability of the partial pressure **of** CO₂ (pCO₂)
12 that is due to the natural carbon cycle using a regional model forced with realistic climate and
13 pre-industrial atmospheric pCO₂ for 1948-2009. Large-scale patterns of natural pCO₂ variability
14 are primarily associated with basin-averaged sea surface temperature (SST) that, in turn, is
15 composed of two parts: the Atlantic Multidecadal Oscillation (AMO) and a long-term positive
16 SST trend. The North Atlantic Oscillation (NAO) drives a secondary mode of variability. For the
17 primary mode, positive AMO and the SST trend modify pCO₂ with different mechanisms and
18 spatial patterns. Positive AMO is also associated with a significant reduction in dissolved
19 inorganic carbon (DIC) in the subpolar gyre, due primarily to reduced vertical mixing; the net
20 impact of positive AMO is to reduce pCO₂ in the subpolar gyre. Through direct impacts on SST,
21 | the net **effect** of positive AMO is to increase pCO₂ in the subtropical gyre. From 1980 to present,
22 long-term SST warming has amplified AMO impacts on pCO₂.

Melissa 4/18/2016 6:56 PM

Deleted: impacts

1 Introduction

To date, the ocean has removed approximately 1/3 of all anthropogenic carbon emitted to the atmosphere and has, thus, substantially damped climate warming (Khatiwala et al., 2009; Sabine et al., 2004). As carbon dioxide emissions continue to increase due to fossil fuel emissions and cement production, there is significant interest in better understanding the ocean carbon cycle. Due to the limited instrumental record and sparse data, multidecadal variability of the ocean carbon sink remains poorly constrained. The North Atlantic, in particular, is a region of highly concentrated carbon uptake (Takahashi et al., 2009) and of significant carbon cycle variability related to variations in the climate, with multiple studies finding an association with the North Atlantic Oscillation (Fay and McKinley, 2013; Schuster et al., 2013; Terry, 2012; Levine et al., 2011; McKinley et al., 2011; Loptien and Eden, 2010; Ullman et al., 2009; Thomas et al., 2008). However, data are sparse, processes are complex and the timescales for studies have differed, and this has complicated a clear elucidation of the mechanisms of North Atlantic carbon cycle variations.

Schuster et al. (2009) analyzed in situ $p\text{CO}_2$ measurements, and suggested a substantial decline in North Atlantic carbon uptake from the mid-1990's to the mid-2000's. LeQuéré et al. (2010) also interpreted observations and models to conclude that there had been a decline in the North Atlantic sink from 1981-2007 due to changing wind patterns and increasing SST. Metzl et al. (2010) focused on subpolar surface ocean carbon cycle changes between 1993-2008, and also concluded that there had been a reduction in carbon uptake. In situ $p\text{CO}_2$ measurements have also been synthesized to illustrate the strong sensitivities of such changes to the locations and timeframe chosen for the analyses (Fay and McKinley 2013; McKinley et al., 2011). The substantial spatial heterogeneity and temporal variability in the North Atlantic complicates efforts to use sparse observations to quantify carbon uptake. Thus, the magnitude and mechanisms affecting North Atlantic carbon cycle variability remain loosely constrained. The present study takes advantage of the full spatial and temporal coverage of a regional numerical model to gain new insights into the mechanisms of variability of North Atlantic $p\text{CO}_2$.

As shown by Ullman et al. (2009) in a 15-year simulation (1992-2006), internal variability in the North Atlantic is partially obscured by the large, quasilinear trend of CO_2 flux into the ocean that is driven by increasing CO_2 emissions. To examine the carbon sink variability that is partially masked by this large carbon influx, we use a hindcast model from 1948-2009

Melissa 4/18/2016 6:38 PM

Deleted: s

forced with the preindustrial atmospheric CO₂ concentration and realistic climate. As described below, we find that the basin-average SST is associated with the leading mode of surface ocean pCO₂ variability. This SST signal, in turn, includes an upward trend due to greenhouse gas emissions and a signal of internal variability characterized by the Atlantic Multidecadal Oscillation (AMO, Kerr, 2000).

2 Methodology

2.1 Physical-Biogeochemical-Ecosystem Model

The MIT Ocean General Circulation Model (Marshall et al., 1997a, 1997b) has been regionally configured for the North Atlantic between 20°S and 81.5°N (Bennington et al., 2009; Ullman et al., 2009). The model has a horizontal resolution of 0.5° latitude and 0.5° longitude and 23 vertical levels beginning with a resolution of 10m thickness at the surface and increasing to 500 m thickness at depths greater than 2200 m. The Gent-McWilliams (Gent and McWilliams, 1990) eddy parameterization and the KPP boundary layer mixing scheme (Large et al., 1994) were employed to model sub-grid-scale processes. Daily fields from NCEP/NCAR Reanalysis I force the model from 1948-2009 (Kalnay et al., 1996). SST and SSS are relaxed to monthly historical SST (HadISSTv1.0, Rayner et al., 2003) and climatological SSS (Antonov et al., 2006) observations, on the timescale of two and four weeks, respectively. Glacier melt and/or river discharge are not included in the model forcing, instead the SSS relaxation approximates these impacts. Freshwater (evaporation – precipitation) forcing and SSS relaxation impacts both salinity and tracer concentrations. In lieu of an active sea ice simulation, observed fractional ice from NCEP Reanalysis 1 is applied with interpolation to daily resolution. For open boundary conditions, a sponge layer exists at 20S, and over the first 5 degrees of latitude to the North, there is restoration to climatological temperature, salinity, DIC and phosphate fields. For temperature and salinity, there is also a sponge layer at Gibraltar. More discussion of the sponge layer can be found in Ullman et al., 2009.

The pelagic ecosystem is parameterized using one zooplankton class and two phytoplankton classes (diatoms and ‘small’ phytoplankton) as described previously (Dutkiewicz et al., 2005; Bennington et al., 2009; Ullman et al., 2009). Carbon (inorganic and dissolved, and particulate organic), alkalinity (ALK), phosphorus, silica and iron cycling are explicitly included in the biogeochemical model. Carbonate chemistry is modeled as in Follows et al. (2006). The objective of this simulation is to identify climate impacts on the natural carbon cycle without the

1 complication of the large CO₂ flux into the ocean that is observed. Thus, atmospheric pCO₂ is
2 fixed at a constant, preindustrial level of 278 ppmv.

3 The physical model was spun up for 100 years. The observed meteorological forcing for
4 1948-1978 was cycled three times (90 years), and then 1948 was repeated 10 years prior to
5 beginning the simulation analyzed here. Following the physical spinup, the biogeochemical
6 model was initialized using preindustrial estimates for DIC and ALK climatology from the
7 GLODAP database (Key et al., 2004). The biogeochemical model was then spun up for an
8 additional 100 years, long enough to eliminate drift in the biogeochemical parameters. The
9 percent change over the last five years of spinup in the basin-averaged surface DIC field is
10 0.00046% per year. For comparison, the percent change in DIC from a high AMO (1955) to low
11 AMO (1975) is .012% per year, two orders of magnitude greater than drift at the end of the spin
12 up. This indicates that a 100-year biogeochemical spinup is sufficient to eliminate model drift
13 that would impact our upper ocean analysis. Following spinup, the model was then run with
14 NCEP/NCAR daily forcing fields for 1948-2009.

15 Model physics across the North Atlantic, as well as pCO₂, DIC and ALK at the Bermuda
16 Atlantic Time Series (Bates, 2007) and in the subpolar North Atlantic have been compared to
17 results from a previous simulation using the same model forced with observed atmospheric pCO₂
18 for 1992-2006 (Ullman et al., 2009). Comparison of this simulation to estimates of the pre-
19 industrial vertical profile of DIC in the subpolar gyre indicates good performance by the model
20 (Supplementary Figure 1 and text). Mikaloff-Fletcher et al. (2007) estimated the pre-industrial,
21 or ‘natural’, air-to-sea CO₂ flux in the North Atlantic with an ocean inversion that incorporated
22 climatological circulations estimated from 10 ocean circulation models. For the North Atlantic
23 from 0° to 75°N, they find an uptake of 0.27±0.07 PgC/yr. The mean natural CO₂ flux averaged
24 over the same spatial domain in our simulation is consistent, 0.23 PgC/yr. In total, our
25 comparison to available data indicate that the model is capable of robustly simulating the carbon
26 biogeochemistry of the North Atlantic and its response to climate variability.

27 2.2 Post-processing

28 CO₂ flux into the ocean is proportional to the partial pressure difference between the
29 atmosphere and ocean surface: $\Delta p\text{CO}_2 = p\text{CO}_2^{\text{atm}} - p\text{CO}_2^{\text{ocean}}$. In this analysis, we can directly
30 relate higher pCO₂^{ocean} to a reduction in CO₂ flux, since atmospheric pCO₂ is fixed. $\Delta p\text{CO}_2$
31 variability sets the sign and magnitude of flux changes on both seasonal and interannual

Melissa 4/18/2016 5:42 PM

Formatted: Font:(Default) +Theme Body

Melissa 4/18/2016 5:42 PM

Formatted: Font:(Default) +Theme Body

Melissa 4/18/2016 7:04 PM

Deleted: with

Melissa 4/18/2016 7:05 PM

Deleted: is

Melissa 4/18/2016 7:05 PM

Deleted:

timescales (Takahashi et al. 2009, Watson et al. 2009, LeQuéré et al. 2010). $p\text{CO}_2$ is decomposed into contributions from temperature and chemical effects using model output and the full carbonate equations (Follows et al., 2006). As in Ullman et al. (2009), $p\text{CO}_2$ -SST is found by allowing only SST to vary in the full carbonate equations for $p\text{CO}_2$, i.e. all other variables (DIC, ALK, SSS, phosphate, silica) are held constant at their long-term mean values; $p\text{CO}_2$ -chem is found by holding SST constant and allowing the rest of the input variables to vary; for $p\text{CO}_2$ -DIC, only DIC varies.

Model diagnostics for DIC are the monthly mean tendency terms (in $\text{mmol/m}^3/\text{yr}$) due to individual modeled processes and are calculated at each time step during the model simulation (Ullman et al., 2009). Monthly mean diagnostics for the surface layer DIC change due to horizontal and vertical advection and diffusion, net biological processes (primary production and respiration), freshwater input/removal, and air-sea CO_2 flux are used.

The AMO index for the model is calculated using modeled SST and observed global Had1SSTv1.0 (Rayner et al., 2003) using the approach of Wang and Dong (2010). This approach regresses the area-weighted global mean Had1SST time series onto area-weighted basin-wide mean North Atlantic SST time series (NASST). This regressed index is subtracted from the total NASST to define the AMO. The combined SST signal is, thus, decomposed into contributions from globally increasing SST (SST trend) and the internal variability of the AMO (Figure 1d). In order to focus on the decadal timescale variability, all timeseries are smoothed with a standardized 121-month box smoother.

3 Results

3.1 Multidecadal Variability

To determine the leading mode of variability in surface ocean $p\text{CO}_2$, principle component analysis is employed. The first empirical orthogonal function (EOF1) patterns and smoothed principle components (PCs) for monthly, 13-month smoothed total $p\text{CO}_2$ and the SST contribution to $p\text{CO}_2$ ($p\text{CO}_2$ -SST) are shown in Figure 1a-c. To determine the change in $p\text{CO}_2$ anomalies described by EOF1 at a specific point in time, the value of the PC1 at that time can be multiplied by the EOF1 pattern. The percent of variance in the total field explained by the EOF1 pattern is 18% and 38% for $p\text{CO}_2$ and $p\text{CO}_2$ -SST, respectively. In both cases, the EOF1 patterns are statistically distinct from their EOF2 patterns, which are discussed in section 4. This EOF analysis unveils the basin-scale coherent variability. There is remaining variability in coherent

secondary large-scale modes (e.g. EOF2) or at scales smaller than the whole basin. That large-scale modes of climatic variability tend to capture 10-40% of variance has been documented across many climate variables, including global SST and tropospheric winds (von Storch and Zwiers, 1999), Southern Ocean geopotential heights (Thomson and Wallace, 2000), and pCO₂ throughout the Pacific (McKinley et al. 2004, 2006). That EOF1 of pCO₂ captures the patterns of multi-decadal large-scale change is further evidenced by plots of 20-year anomalies of pCO₂ (Figure S2).

The correlation between PC1-pCO₂ and the area-weighted basin-averaged SST is 0.88 (Figure 1c, Table S1). An increase in temperature increases pCO₂ by reducing solubility, which is illustrated by the pCO₂-SST EOF1 pattern. PC1- pCO₂ and PC1- pCO₂-SST are highly correlated (Figure 1c, $r = 0.91$), but have distinct EOF1 patterns, particularly in the subpolar gyre (Figure 1a,b). This is consistent with the pCO₂ in the subpolar gyre also being significantly impacted by changes in DIC supply which in turn, are associated with the AMO. EOF1 for pCO₂-chem and pCO₂-DIC explain 32% and 25% of the variance, respectively (Figure 2a,b), and these PC1's are highly correlated with the AMO, $r = 0.99, 0.96$, respectively (Figure 2d, Table S1).

Alkalinity can also affect pCO₂-chem since increased alkalinity reduces pCO₂. PC1 for EOF1 of pCO₂-ALK (Figure 2c) does not correlate highly to PC1's of total pCO₂ or pCO₂-chem ($r = -0.25$; $r = 0.44$, respectively), or to the AMO (see supplementary table 1). Though alkalinity does contribute to the spatial pattern shown in the EOF1 of pCO₂-chem, the temporal evolution of this pattern differs substantially and is not strongly connected to the AMO or to EOF1 of pCO₂. Therefore, we focus on the more direct relationship between pCO₂-DIC and pCO₂-chem for the rest of the paper, and reserve the alkalinity relationships for future in-depth analysis.

The AMO, an index of internal North Atlantic SST variability, declines (cools) until 1975 and rises thereafter (Figure 1d). Taking the last half of the timeseries as an example, increasingly positive AMO corresponds to a decrease in pCO₂-chem, with the strongest declines in the subpolar gyre and driven by reduced pCO₂-DIC (Figure 2). This occurs in opposition to the direct effect on pCO₂ of warmer NASST (Figure 1b,c), driven jointly by the increasingly positive AMO and the warming trend (Figure 1d). SST and chemical terms vary inversely because higher SST (AMO+) enhances stratification, leading to a shoaling of mixed layer depths over most of the gyre (discussed in section 4). This shoaling in turn limits the amount of deep, carbon-rich

Melissa 4/18/2016 7:09 PM

Deleted: EOF1

Melissa 4/18/2016 5:26 PM

Deleted:

Melissa 4/18/2016 7:24 PM

Deleted: gyre (Figure S2

Melissa 4/18/2016 7:24 PM

Deleted:)

water that is mixed to the surface, reducing pCO₂-DIC and pCO₂-chem (Ullman et al., 2009). The correlation of PC1-pCO₂-chem and PC1-pCO₂-DIC with PC1-pCO₂-SST are 0.90 and 0.91, respectively (Table S1). Mechanisms of AMO impacts on pCO₂-chem in the subpolar gyre will be explored further below.

3.2 Regression Analysis

Regression of the AMO, SST trend, and total SST (Figure 1d) onto monthly pCO₂, pCO₂-SST and pCO₂-chem further illustrates that temperature and chemical responses tend to act in opposition to one another, damping total pCO₂ responses across the basin (Figure 3). This analysis compliments the above EOF analysis by allowing the use of the same index of temporal variability across all fields. Previous studies with observations and models have shown that pCO₂-chem dominates the seasonality of pCO₂ in the subpolar gyre, via strong vertical supply of DIC in winter that drives up pCO₂ and biological DIC drawdown in summer that ~~reduces~~ pCO₂. Temperature impacts oppose these seasonal oscillations, but are of weaker amplitude (Kortzinger et al. 2008; Takahashi et al. 2002). Models have shown similar opposing influences with respect to interannual variability (Ullman et al. 2009; McKinley et al. 2004). These regressions illustrate that positive AMO leads to higher pCO₂-SST throughout the basin (Figure 3b). The response is strongest north of 35°N with a clear maximum to the east of Newfoundland. Simultaneously, positive AMO is associated with a reduction in pCO₂-chem (Figure 3c). The pCO₂-chem signal is also strongest to the north. The overall effect is a decrease in total pCO₂ north of 45°N and a slight increase in pCO₂ in the eastern subtropical gyre (Figure 3a).

When responding to the global SST trend, pCO₂-SST more heavily controls the response of the total pCO₂ field (Figure 3d,e). The pCO₂-SST response is strongest along the Gulf Stream and east of Newfoundland, and also increases somewhat off the coast of Europe and Africa. pCO₂-chem exhibits some decline in the Gulf Stream region, and has a small response elsewhere (Figure 3f).

Regression with the total NASST timeseries (Figure 1) illustrates the combined effects of the AMO and trend signals (Figure 3g-i). A positive anomaly of NASST depresses total pCO₂ in the subpolar gyre, consistent with the AMO impact found above. Positive NASST also increases total pCO₂ off North Africa, consistent with the impact of the SST trend. pCO₂-SST increases both off Africa and has a strong maximum in the Gulf Stream region east of Newfoundland with

Melissa 4/18/2016 7:29 PM

Deleted: drives

Melissa 4/18/2016 7:29 PM

Deleted: down

positive NASST anomalies. The $p\text{CO}_2$ -chem response is slightly weaker in the subpolar gyre than for the AMO alone (Figure 3a,i).

3.3 DIC Diagnostics

To further investigate the chemical term response to the AMO, model diagnostics for the DIC field are regressed upon the AMO index. Diagnostics are modeled rates of change in DIC due to one of five processes that have been saved at every model time-step. Physical processes are separated into horizontal advection and diffusion (DIC-horz), and vertical advection and diffusion (DIC-vert). DIC-phys is the sum of vertical and horizontal transport, showing the net effect of physical transport on DIC (Figure 4). The rate of DIC supply is also affected by biological processes involving DIC incorporation into organic matter and remineralization back to inorganic (DIC-bio), net precipitation/evaporation that dilutes or concentrates DIC (DIC-fresh) and the air-sea flux of CO_2 (DIC-flx) (Figure 5). The focus on DIC is justified by the fact that $p\text{CO}_2$ -chem change has the same pattern and is highly correlated with $p\text{CO}_2$ -DIC change (Figure 2). The focus on the AMO is justified by its strong imprint on $p\text{CO}_2$ through $p\text{CO}_2$ -chem (Figure 2, 3).

For the long-term average, vertical advection and diffusion are positive along the Gulf Stream and in the subpolar gyre due to deep winter mixed layer depths (MLD) that mix up high-DIC water from below (Figure 4a). Horizontal DIC advection and mixing removes this vertically supplied DIC along the Gulf Stream and in the western subpolar gyre (Figure 4b). While the vertical and horizontal components tend to have opposing influences, the net effect is a positive DIC supply to the subpolar gyre, as shown by mean DIC-phys (Figure 4c). With positive AMO, vertical advective and diffusive fluxes of DIC decrease in the Irminger Sea and Iceland basin, while they increase in the Labrador Sea and east of Newfoundland (Figure 4d). These changes are consistent with AMO-related MLD changes outside of the Labrador Sea (Figure 6) and change in the basin-scale barotropic streamfunction indicating a weakened subpolar gyre (Figure 7). The effect of this is to shift the central DIC-vert maximum to the west. With positive AMO, horizontal advection and diffusion largely respond to changes in vertical advection and diffusion, with less horizontal divergence (a positive change) in regions where the vertical supply is reduced (Figure 4e). The net effect shown by DIC-phys reveals an overall reduction in DIC supply (Figure 4f), consistent with a weaker subpolar gyre circulation and shallower MLDs that reduce the vertical supply of DIC. Hakkinen and Rhines (2009) illustrate and increased

Melissa 4/18/2016 7:31 PM

Deleted: 5

Melissa 4/18/2016 7:31 PM

Deleted: 6

1 penetration of subtropical waters into the subpolar region from the 1990s to the 2000s, consistent
2 with a weaker subpolar gyre circulation. The changes in MLD and streamfunction are also in
3 agreement with results from Zhang (2008) who links the observed spindown of the subpolar gyre
4 in the 1990's to an enhanced MOC using a combination of satellite altimeter observations and
5 results from a 1000-year coupled ocean-atmosphere model simulation.

6 Mean DIC impacts from physics, biological processes, freshwater and air-sea flux are
7 shown in Figure 5a-e. The net impact of biology is to remove DIC from the surface of most of
8 the region, with the most intense removal along the Gulf Stream (Figure 5a). The smaller impact
9 of evaporation and precipitation is to concentrate DIC in the subtropics and to dilute it in the
10 subpolar gyre (Figure 5b). The air-sea CO₂ flux term is also small, positive north of about 35°N
11 and negative to the south (Figure 5c). AMO-related change in the biological removal of DIC
12 indicates additional removal (negative anomaly) occurring in the same region where horizontal
13 flux increases, consistent with biological stimulation through an increased supply nutrients from
14 the subtropical subsurface along the “nutrient stream” (Williams et al., 2006). There is reduced
15 biological productivity, and thus a reduction of DIC loss (a positive DIC anomaly), in other parts
16 of the basin that are consistent with satellite observations from the late 1990s to the mid-2000s
17 (Behrenfeld et al. 2006). Changes in surface ocean DIC content due to freshwater fluxes and air-
18 sea CO₂ flux with the AMO are small. Across the basin, the net DIC change associated with
19 AMO is negative, with the strongest negative changes occurring in the subpolar gyre (Figure 2b,
20 3c)

21 4 Discussion and Conclusions

22 In this North Atlantic regional model forced with pre-industrial pCO₂ and realistic
23 climate from 1948-2009, SST is the dominant driver of pCO₂ variability, with both long-term
24 anthropogenic warming and the AMO playing important roles. The AMO strongly influences
25 chemical change, which in turn is mostly driven by DIC. DIC changes, in turn, are due primarily
26 to changes in vertical and horizontal advection and mixing. Changing biology has the most
27 important secondary effect, and largely damps the anomalies caused by advection and mixing.
28 Freshwater and CO₂ fluxes changes are slight.

29 Our findings linking the AMO to natural carbon cycle variability in the North Atlantic are
30 consistent with the study of Séférian et al. (2013) who also found an AMO-like signal dominated
31 North Atlantic pCO₂ variability in a 1000-year Earth System Model simulation with constant

Melissa 4/18/2016 7:33 PM

Deleted: 7a

Melissa 4/18/2016 7:33 PM

Deleted: 7a

Melissa 4/18/2016 7:33 PM

Deleted: 7b

Melissa 4/18/2016 7:33 PM

Deleted: 7c

Melissa 4/18/2016 5:27 PM

Formatted: Font:(Default) +Theme Body

1 pCO₂. Other studies have focused on the relationship between the North Atlantic Oscillation
2 (NAO) and CO₂ flux using models and observations (Loptien and Eden 2010; Ullman et al.
3 2009; Schuster et al., 2009; Thomas et al., 2008). Consistent with these previous studies, the
4 NAO is the second mode of variability in this simulation (Figure S4, S5), and the corresponding
5 principle components are highly correlated with the NAO (Table S2). The shorter timeframe for
6 most previous studies explains, in part, the difference in attribution to the AMO as opposed to
7 NAO. Our results are broadly consistent with previous studies in the finding that physical
8 variability is the dominant driver of variability in the North Atlantic surface ocean carbon cycle.

9 The NAO and AMO may, in fact, be linked through the Meridional Overturning
10 Circulation (MOC), with a positive NAO enhancing MOC, which over time warms SSTs and
11 leads to a positive AMO. Stronger overturning (enhanced MOC) may result in positive SST
12 anomalies and thus a positive AMO phase over time, with some lag between the peak MOC and
13 peak AMO response. Latif et al. 2004 used a model to show that oceanic heat transport related
14 to the MOC leads the SST response (potentially the AMO) by about 10 years, while Delworth
15 and Mann (2000) found a 10-year lag between subsurface temperature anomalies and MOC. The
16 precise mechanisms remain in debate due to different model findings and a lack of observational
17 constraints (Delworth & Mann, 2000; Knight et al., 2005; Dima & Lohmann, 2007; Latif et al.,
18 2006; Kavvada et al., 2013 and references therein). In our simulation, the NAO and MOC are
19 significantly correlated ($r = 0.57$, Table S1) and there is also a high correlation ($r = 0.86$)
20 between the NAO (Figure S3) and the 15-year lagged AMO. These correlations are broadly
21 consistent with the above-postulated NAO-MOC-AMO relationship. On the other hand, Booth et
22 al. (2012) suggest that the AMO may be driven, in fact, by atmospheric aerosol variability, so it
23 is possible that there is no such AMO/MOC relationship at all. Future modeling and
24 observations should further elucidate these connections which reach beyond the scope of this
25 study.

26 We find multidecadal variability in the natural carbon cycle of the surface North Atlantic
27 to be dominated by an SST trend and multidecadal SST variations captured by the AMO index.
28 Variability linked to the AMO influences both pCO₂-SST and pCO₂-chem. In the subpolar gyre,
29 the positive SST influence on pCO₂ is overwhelmed by reduced supply of DIC to the surface
30 ocean through mixing and advection, the net impact being reduced pCO₂. The reduction in
31 mixing is associated with shoaling of MLDs and a weaker subpolar gyre circulation, both

Melissa 4/18/2016 5:45 PM
Formatted: Font:(Default) +Theme Body

Melissa 4/18/2016 5:45 PM
Formatted: Font:(Default) +Theme Body

Melissa 4/18/2016 5:45 PM
Formatted: Font:(Default) +Theme Body

Melissa 4/18/2016 5:45 PM
Formatted: Font:(Default) +Theme Body

Melissa 4/18/2016 5:45 PM
Formatted: Font:(Default) +Theme Body

Melissa 4/18/2016 5:45 PM
Formatted: Font:(Default) +Theme Body

Melissa 4/18/2016 5:45 PM
Formatted: Font:(Default) +Theme Body

Melissa 4/18/2016 5:45 PM
Formatted: Font:(Default) +Theme Body

Melissa 4/18/2016 5:45 PM
Formatted: Font:(Default) +Theme Body

Melissa 4/18/2016 5:45 PM
Formatted: Font:(Default) +Theme Body

Melissa 4/18/2016 6:49 PM
Formatted: Font:(Default) +Theme Body

Melissa 4/18/2016 6:49 PM
Formatted: Font:(Default) +Theme Body

Melissa 4/18/2016 6:49 PM
Formatted: Font:(Default) +Theme Body

Melissa 4/18/2016 5:31 PM
Deleted: this

Melissa 4/18/2016 5:51 PM
Formatted: Font color: Auto

Melissa 4/18/2016 5:29 PM
Deleted: ,

Melissa 4/18/2016 5:29 PM
Deleted: direct AMO-MOC relationship

Melissa 4/18/2016 7:40 PM
Deleted: the

associated with warmer SSTs (positive AMO). In the subtropics, the SST impact is stronger and thus pCO₂ is increased under the influence of positive AMO and positive SST trend.

These findings are consistent with observed relationships between trends in surface ocean pCO₂ and trends in atmospheric pCO₂ since the 1980s (Fay and McKinley, 2013). In the North Atlantic subpolar gyre, trends in surface ocean pCO₂ lagged the trend in atmospheric pCO₂ from the early to mid 1990s to the late 2000s, which is consistent with the AMO and the SST trend reducing DIC supply to the subpolar gyre as found in this study. On smaller spatial scales and shorter timeframes, trends in ocean pCO₂ can differ (Fay and McKinley, 2013; Metzl 2010, Watson et al 2009, Schuster et al. 2009), which can be reasonably attributed to shorter-term and smaller spatial scale variability. We also find that warming has contributed to the observed pCO₂ increase from the 1980-90s through the 2000s throughout the basin. These model results allow a mechanistic attribution of these observed changes in North Atlantic pCO₂ to the combined effect of the AMO and a positive SST trend due to anthropogenic climate change.

Acknowledgements

The authors are grateful for support from NASA grants (NNX/11AF53G, and NNX/13AC53G). Model code is freely available at MITgcm.org; model fields analyzed here can be acquired by contacting GAM.

References

- Antonov, J. I., R. A. Locarnini, T. P. Boyer, A. V. Mishonov, and H. E. Garcia (2006), World Ocean Atlas 2005 vol. 2, Salinity, NOAA Atlas NESDIS 62, edited by S. Levitus, 182 pp., U.S. Govt. Print. Off., Washington, D. C..
- Bates, N. R (2007), Interannual variability of the oceanic CO₂ sink in the subtropical gyre of the North Atlantic Ocean over the last 2 decades, *J. Geophys. Res.*, 112, C09013, doi:10.1029/2006JC003759.
- Behrenfeld, M. J., R. T. O'Malley, D. A. Siegel, C. R. McClain, J. L. Sarmiento, G. C. Feldman, A. J. Milligan, P.G. Falkowski, R. M. Letelier, E. S. Boss (2006), Climate-driven trends in contemporary ocean productivity. *Nature* **444**, 752–755.

1 Bennington, V., G. A. McKinley, S. Dutkiewicz, and D. Ullman (2009), What does chlorophyll
2 variability tell us about export and CO₂ flux variability in the North Atlantic?, *Global*
3 *Biogeochem. Cycles*, 23, GB3002, doi:10.1029/2008GB003241.

4 Booth, B. B. B., N. J. Dunstone, P. R. Halloran, T. Andrews, N. Bellouin (2012), Aerosols
5 implicated as a prime driver of twentieth-century North Atlantic climate variability. *Nature*,
6 **484**, 228-232, doi:10.1038/nature10946.

7 Delworth, T. L., and M. E. Mann (2000), Observed and simulated multidecadal variability in the
8 Northern Hemisphere, *Clim. Dyn.*, 16, 661–676, doi:10.1007/s003820000075.

9 Dima, M, and G. Lohmann (2007), A Hemispheric Mechanism for the Atlantic Multidecadal
10 Oscillation, *J. Climate*, 20, 2706-2718, DOI: 10.1175/JCLI4174.1.

11 Dutkiewicz, S., M. J. Follows, and P. Parekh (2005), Interactions of the iron and phosphorus
12 cycles: A three-dimensional model study, *Global Biogeochem. Cycles*, 19, GB1021,
13 doi:10.1029/2004GB002342.

14 Fay, A. R., and G. A. McKinley (2013), Global trends in surface ocean pCO₂ from in situ data,
15 *Global Biogeochem. Cycles*, 27, doi:10.1002/gbc.20051.

16 Follows, M. J., S. Dutkiewicz, and T. Ito (2006), On the solution of the carbonate system in
17 ocean biogeochemistry models, *Ocean Modell.*, 12, 290–301,
18 doi:10.1016/j.ocemod.2005.05.004.

19 Gent, P. R., and J. C. McWilliams (1990), Isopycnal mixing in ocean general circulation models ,
20 *J. Phys. Oceanogr.*, 20, 150–155.

21 Hakkinen, S., and P. B. Rhines (2009), Shifting surface currents in the northern North Atlantic
22 Ocean, *J. Geophys. Res.*, 114, C04005, doi:10.1029/2008JC004883.

23 Key, R. M., R. M. Key, A. Kozyr, C. L. Sabine, K. Lee, R. Wanninkhof, J. L. Bullister, R. A.
24 Feely, F. J. Millero, C. Mordy , T.-H. Peng (2004), A global ocean carbon climatology:
25 Results from Global Data Analysis Project (GLODAP), *Global Biogeochem. Cycles*, 18,
26 GB4031, doi:10.1029/2004GB002247.

1 Kalnay, E., M. Kanamitsu, R. Kistler, W. Collins, D. Deaven, L. Gandin, M. Iredell, S. Saha, G.
2 White, J. Woollen, Y. Zhu, A. Leetmaa, R. Reynolds, M. Chelliah, W. Ebisuzaki, W. Higgins,
3 J. Janowiak, K. C. Mo, C. Ropelewski, J. Wang, R. Jenne, and D. Joseph (1996), The
4 NCEP/NCAR 40-Year Reanalysis Project, Bull. Amer. Meteor. Soc., 77, 437–471,
5 doi: [http://dx.doi.org/10.1175/1520-0477\(1996\)077<0437:TNYRP>2.0.CO;2](http://dx.doi.org/10.1175/1520-0477(1996)077<0437:TNYRP>2.0.CO;2).

6 [Kavvada, A. A. Ruiz-Barradas and S. Nigam \(2013\), AMO's structure and climate footprint in](#)
7 [observations and IPCC AR5 climate simulations, *Climate Dynamics*, **41-5**, 1345-1364.](#)

8
9 Kerr, R. A. (2000), A North Atlantic Climate Pacemaker for the Centuries, Science, 288, 1984-
10 1985, doi:10.1126/science.288.5473.1984.

11
12 Khatiwala, S., F. Primeau, and T. Hall (2009), Reconstruction of the history of anthropogenic
13 CO₂ concentrations in the ocean, Letters to Nature, 462, 346-349, doi:10.1038/nature08526.

14
15 Knight, J. R., R. J. Allan, C. K. Folland, M. Vellinga, and M. E. Mann (2005), A signature of
16 persistent natural thermohaline circulation cycles in observed climate, Geophys. Res. Lett.,
17 32, L20708, doi:10.1029/2005GL024233.

18 Körtzinger, A., U. Send, R. S. Lampitt, S. Hartman, D. W. R. Wallace, J. Karstensen, M. G.
19 Villagarcia, O. Llinás, and M. D. DeGrandpre (2008) The seasonal pCO₂ cycle at
20 49°N/16.5°W in the northeastern Atlantic Ocean and what it tells us about biological
21 productivity. *J. Geophys. Res.* **113**, C04020.

22 Large, W. G., J. C. McWilliams, and S. C. Doney (1994), Oceanic vertical mixing: A review and
23 a model with a nonlocal boundary layer parameterization, Rev. Geophys., 32, 363–403.

24 [Latif, M., E. Roeckner, B. Botzet, M. Esch, H. Haak, S. Hagemann, J. Jungclauss, S. Legutke, S.](#)
25 [Marsland, and U. Mikolajewicz \(2004\), Reconstructing, Monitoring, and Predicting](#)
26 [Multidecadal-Scale Changes in the North Atlantic Thermohaline Circulation with Sea](#)
27 [Surface Temperature, *J. Climate*, 17:7, 1605-1614. DOI: \[http://dx.doi.org/10.1175/1520-\]\(http://dx.doi.org/10.1175/1520-0442\(2004\)017<1605:RMAPMC>2.0.CO;2\)](#)
28 [0442\(2004\)017<1605:RMAPMC>2.0.CO;2](#),

Melissa 4/18/2016 5:58 PM

Formatted: Font:Not Bold

Melissa 4/18/2016 5:58 PM

Formatted: Font:Bold

Melissa 4/18/2016 6:41 PM

Formatted: Tabs:Not at 0.19"

Melissa 4/18/2016 5:56 PM

Formatted: Font:Not Bold

Melissa 4/18/2016 5:55 PM

Formatted: Font:Italic

Melissa 4/18/2016 5:56 PM

Formatted: Font:(Default) +Theme Body, 12 pt, Not Italic

Melissa 4/18/2016 5:56 PM

Formatted: Font:(Default) +Theme Body, 12 pt, Not Italic

Unknown

Field Code Changed

Melissa 4/18/2016 5:56 PM

Formatted: Font:+Theme Body, Not Bold

1 Latif, M., C. Böning, J. Willebrand, A. Biastoch, J. Dengg, N. Keenlyside, U. Schweckendiek,
2 and G. Madec (2006), Is the Thermohaline Circulation Changing?, *J. Climate*, 19, 4631–4637,
3 doi: <http://dx.doi.org/10.1175/JCLI3876.1>
4

5 [Levine, N. M., S C Doney, I Lima, R Wanninkhof, N R Bates, and R A Feely. The impact of the](#)
6 [North Atlantic Oscillation on the uptake and accumulation of anthropogenic CO₂ by North](#)
7 [Atlantic Ocean mode waters. *Global Biogeochem Cy* **25**, GB3022 \(2011\).](#)
8

9 Le Quéré, C., Takahashi, T., Buitenhuis, E. T., Rödenbeck, C. & Sutherland, S. C. (2010),
10 Impact of climate change and variability on the global oceanic sink of CO₂, *Global*
11 *Biogeochem Cycles*, 24, GB4007, doi: 10.1029/2009GB003599.
12

13 Löptien, U., and C. Eden (2010), Multidecadal CO₂ uptake variability of the North Atlantic, *J.*
14 *Geophys. Res.*, 115, D12113, doi:10.1029/2009JD012431.

15 Marshall, J. C., A. Adcroft, C. Hill, L. Perelman, and C. Heisey (1997a), A finite volume,
16 incompressible Navier-Stokes model for studies of the ocean on parallel computers, *J.*
17 *Geophys. Res.*, 102, 5753–5766.

18 Marshall, J. C., C. Hill, L. Perelman, and A. Adcroft (1997b), Hydrostatic, quasi-hydrostatic and
19 non-hydrostatic ocean modeling, *J. Geophys. Res.*, 102, 5733–5752.

20 McKinley, G. A., Fay, A. R., Takahashi, T., and Metzl, N. (2011), Convergence of atmospheric
21 and North Atlantic carbon dioxide trends on multidecadal timescales, *Nat. Geosci.*, 4, 606–
22 610, doi:10.1038/Ngeo1193.

23 McKinley, G. A., M. J. Follows, and J. Marshall (2004), Mechanisms of air-sea CO₂ flux
24 variability in the equatorial Pacific and the North Atlantic, *Global Biogeochem. Cycles*, 18,
25 GB2011, doi:10.1029/2003GB002179.

26 McKinley, G. A., T. Takahashi, E. Buitenhuis, F. Chai, J. R. Christian, S. C. Doney, M.-S. Jiang,
27 K. Lindsay, J. K. Moore, C. Le Quéré, I. Lima, R. Murtugudde, L. Shi, and P. Wetzol (2006),

1 North Pacific carbon cycle response to climate variability on seasonal to decadal timescales.
2 J Geophys Res-Oceans, **111**, C07S06, doi: 10.1029/2005JC003173.
3
4 Metzl, N., A. Corbière, G. Reverdin, A. Lenton, T. Takahashi, A. Olsen, T. Johannessen, D.
5 Pierrot, R. Wanninkhof, S. R. Ólafsdóttir, J. Olafsson, M. Ramonet (2010), Recent
6 acceleration of the sea surface $f\text{CO}_2$ growth rate in the North Atlantic subpolar gyre (1993–
7 2008) revealed by winter observations, Global Biogeochem. Cycles, 24, GB4004,
8 doi:10.1029/2009GB003658.
9
10 Mikaloff Fletcher, S. E., N. Gruber, A. R. Jacobson, M. Gloor, S. C. Doney, S. Dutkiewicz, M.
11 Gerber, M. Follows, F. Joos, K. Lindsay, D. Menemenlis, A. Mouchet, S. A. Müller, and J. L.
12 Sarmiento (2007), Inverse estimates of the oceanic sources and sinks of natural CO_2 and the
13 implied oceanic carbon transport, Global Biogeochem. Cycles, 21, GB1010,
14 doi:10.1029/2006GB002751.

15 Rayner, N. A., D. E. Parker, E. B. Horton, C. K. Folland, L. V. Alexander, D. P. Rowell, E.C.
16 Kent, and A. Kaplan (2003), Global analyses of sea surface temperature, sea ice, and night
17 marine air temperature since the late nineteenth century, J. Geophys. Res., 108, 4407,
18 doi:10.1029/2002JD002670.

19 Sabine, C. L., R. A. Feely, N. Gruber, R. M. Key, K. Lee, J. L. Bullister, R. Wanninkhof, C. S.
20 Wong, D. W. R. Wallace, B. Tilbrook, F. J. Millero, T. Peng, A. Kozyr, T. Ono, A. F. Rios
21 (2004), The oceanic sink for anthropogenic CO_2 , Science 305, 367–371.
22 doi: 10.1126/science.1097403.

23 Schuster, U. G. A. McKinley, N. Bates, F. Chevallier, S. C. Doney, A. R. Fay, M. González-
24 Dávila, N. Gruber, S. Jones, J. Krijnen, P. Landschützer, N. Lefèvre, M. Manizza, J. Mathis,
25 N. Metzl, A. Olsen, A. F. Rios, C. Rödenbeck, J. M. Santana-Casiano, T. Takahashi,
26 R. Wanninkhof, and A. J. Watson (2013), An Assessment of the Atlantic and Arctic sea-air-
27 CO_2 fluxes, 1990-2009. Biogeosciences, 10, 607-627, doi:10.5194/bg-10-607-2013.
28 Schuster, U., Watson, A.J., Bates, N., Corbière, A., González- Dávila, M., Metzl, N., Pierrot, D.,
29 and J. M. Santana-Casiano (2009), Trends in North Atlantic sea-surface $f\text{CO}_2$ from 1990 to

1 2006, *Deep Sea Res., Part II*, 56, 620–629, doi:10.1016/j.dsr2.2008.12.011.

2 Séférian, R., Bopp, L., Swingedouw, D. and Servonnat, J. (2013), Dynamical and
3 biogeochemical control on the decadal variability of ocean carbon fluxes. *Earth Syst. Dynam.*
4 4, 109–127, doi:10.5194/esd-4-109-2013.

5 Takahashi, T., Sutherland, S. C., Wanninkhof, R., Sweeney, C., Feely, R. A., Chipman, D. W.,
6 Hales, B., Friederich, G., Chavez, F., Sabine, C., Watson, A., Bakker, D. C. E., Schuster, U.,
7 Metzl, N., Yoshikawa-Inoue, H., Ishii, M., Midorikawa, T., Nojiri, Y., Körtzinger, A.,
8 Steinhoff, T., Hoppema, M., Olafsson, J., Arnarson, T. S., Tilbrook, B., Johannessen, T.,
9 Olsen, A., Bellerby, R., Wong, C. S., Delille, B., Bates, N. R., and de Baar, H. J. W. (2009),
10 Climatological mean and decadal change in surface ocean pCO₂, and net sea-air CO₂ flux
11 over the global oceans, *Deep-Sea Res. II*, 56, 554–577, doi:10.1016/j.dsr2.2008.12.009.

12 Takahashi, T., Sutherland, S. C., Sweeney, C., Poisson, A., Metzl, N., Tilbrook, B., Bates, N.,
13 Wanninkhof, R., Feely, R. F., Sabine, C., Olafsson, J., and Nojiri, Y. (2002). Global sea-air
14 CO₂ flux based on climatological surface ocean pCO₂, and seasonal biological and
15 temperature effects, *Deep-Sea Research II*, 49, 1601-1622.

16 Terry, L. (2012), Evidence for multiple drivers of North Atlantic multi-decadal climate
17 variability. *Geophys. Res. Lett.*, 39, L19712, doi:10.1029/2012GL053046.

18 Thomas, H., F. Prowe, A.E., Lima, I.D., Doney, S.C., Wanninkhof, R., Greatbatch, R.J., Schuster,
19 U., and A. Corbière (2008), Changes in the North Atlantic Oscillation influence CO₂ uptake
20 in the North Atlantic over the past 2 decades, *Global Biogeochem. Cycles*, 22,
21 doi: 10.1029/2007GB003167.

22 Thompson, D. & Wallace, J. M. (2000), Annular modes in the extratropical circulation. Part I:
23 Month-to-month variability. *J Climate*, **13**, 1000–1016.

24 Ullman, D.J., G.A. McKinley, V. Bennington, S. Dutkiewicz (2009), Trends in the North
25 Atlantic carbon sink: 1992-2006, *Global Biogeochem. Cycles*, 23, GB4011,
26 doi:10.1029/2008GB003383.

27

28 Von Storch, H. and F.W. Zwiers (1999) *Statistical Analysis in Climate Research*. Cambridge

1 University Press. 484 pp.

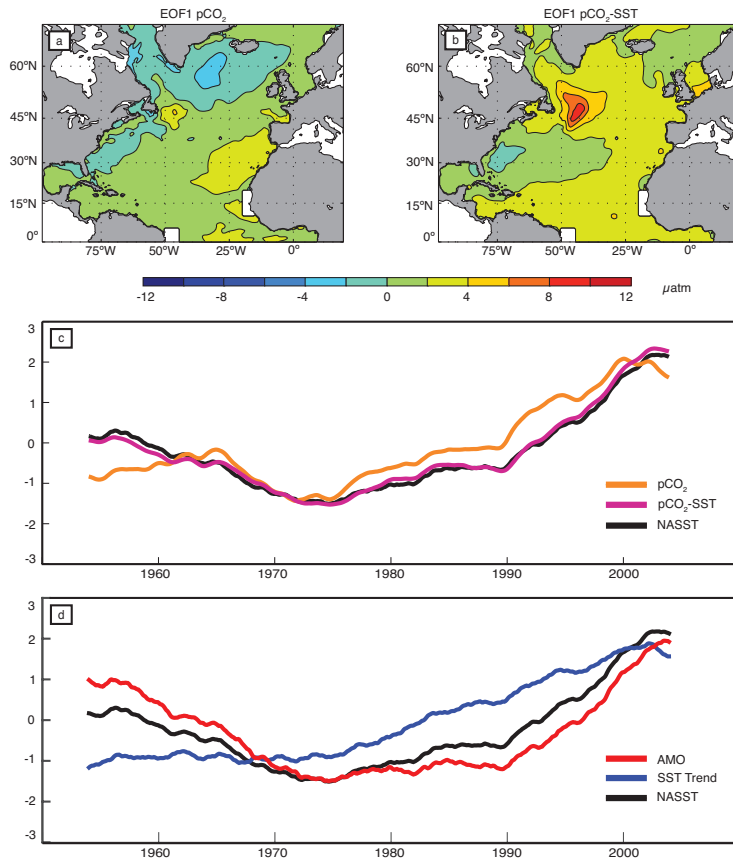
2 Wang, C., and S. Dong (2010), Is the basin-wide warming in the North Atlantic Ocean related to
3 atmospheric carbon dioxide and global warming?, *Geophys. Res. Lett.*, 37, L08707,
4 doi:10.1029/2010GL042743.

5 Watson, A. J., U. Schuster, D. C. E. Bakker, N. R. Bates, A. Corbière, M. González-Dávila, T.
6 Friedrich, J. Hauck, C. Heinze, T. Johannessen, A. Körtziner, N. Metzl, J. Olafsson, A. Olsen,
7 A. Oschlies, X. A. Padin, B. Pfeil, J. M. Santana-Casiano, T. Steinhoff, M. Telszewski, A. F.
8 Rios, D. W. R. Wallace and R. Wanninkhof (2009) Tracking the Variable North Atlantic
9 Sink for Atmospheric CO₂. *Science*, **326**, 1391–1393 DOI: 10.1126/science.1177394.

10 Williams, R. G., V. Roussenov, and M. J. Follows (2006), Induction of nutrients into the mixed
11 layer and maintenance of high latitude productivity, *Global Biogeochem. Cycles*, 20,
12 GB1016, doi:10.1029/2005GB002586.

13 Zhang, R. (2008), Coherent surface-subsurface fingerprint of the Atlantic meridional overturning
14 circulation. *Geophysical Research Letters*, **35**, L20705, doi:10.1029/2008GL035463.

15



1
2 Figure 1: a) EOF1 of total pCO₂ (μatm), b) EOF1 of pCO₂-SST (μatm), explaining 18% and
3 38% of total variance, respectively. c) PC1- pCO₂ (orange), PC1- pCO₂-SST (pink) and area-
4 weighted, basin-averaged standardized North Atlantic SST time series (black), d) Area-weighted,
5 basin-averaged (0-70N, 98W-19.5E) North Atlantic SST from Had1SST (black), global area-
6 weighted SST regressed onto North Atlantic SST (blue), and AMO index created by subtracting
7 the global regression from the North Atlantic SST (red). All indices are standardized by 1-sigma.
8 Timeseries smoothed with a 121-month box smoother. Two small coastal areas off Africa and
9 South America were excluded in a) and b) due to the presence of localized, anomalously strong
10 upwelling in the early 1960's that precluded elucidation of the large-scale pattern.

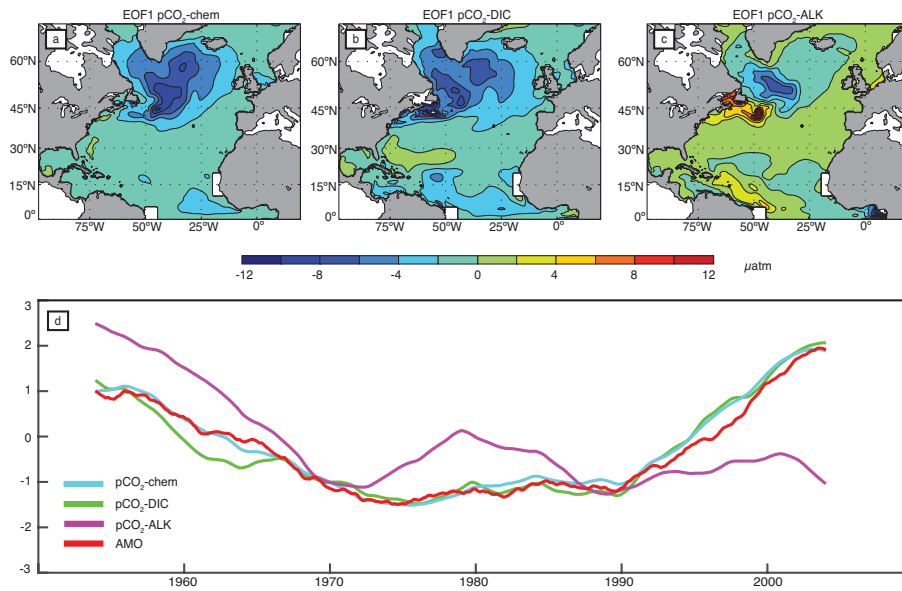


Figure 2: a) EOF1 pCO₂-chem (μatm), b) EOF1 pCO₂-DIC (μatm), c) EOF1 pCO₂-ALK explaining 32%, 25%, and 19% of total variance, respectively, d) PC1- pCO₂-chem (cyan), PC1- pCO₂-DIC (green) PC1- pCO₂-ALK (magenta) and AMO index (red), all standardized. Timeseries smoothed with a 121-month box smoother.

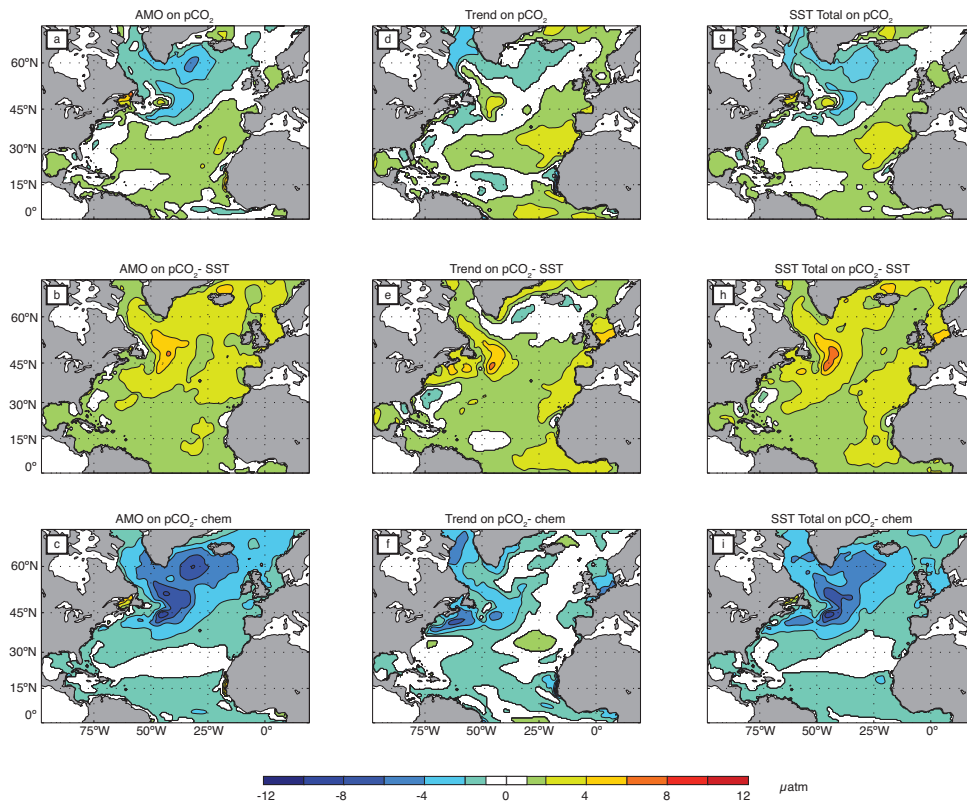


Figure 3: 121-month box-smoothed AMO regressed onto unsmoothed, monthly a) pCO_2 , b) pCO_2 -SST, c) pCO_2 -chem. SST Trend regressed onto d) pCO_2 , e) pCO_2 -SST, f) pCO_2 -chem. NASST (AMO + SST Trend) regressed onto g) pCO_2 , h) pCO_2 -SST, i) pCO_2 -chem. Regressions calculated from 1953 through 2005. Values <0.5 and $>0.5 \mu atm$ are whited out to highlight regions experiencing the most substantial changes.

Melissa 4/18/2016 7:16 PM

Deleted: 3

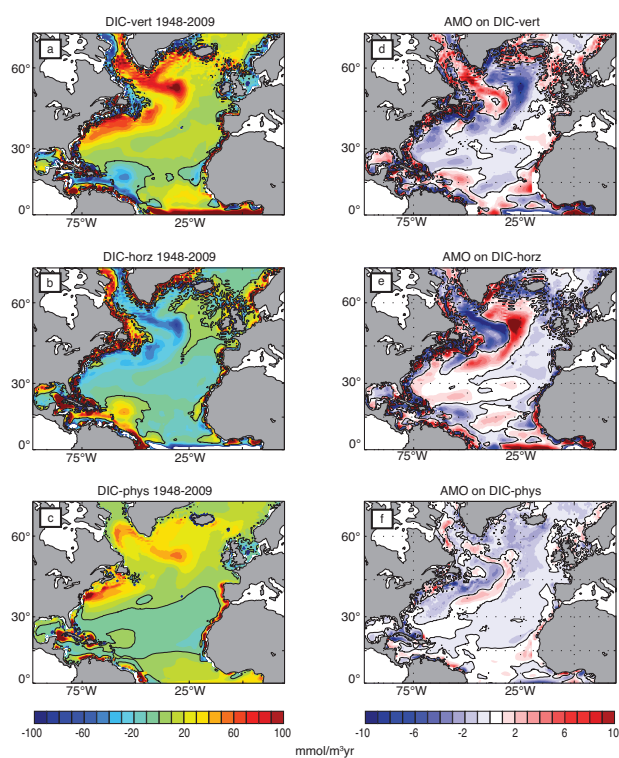


Figure 4: DIC diagnostics. Left column: 1948-2009 Mean a) DIC-vertical, b) DIC-horizontal, c) DIC-physical where DIC-physical is the sum of DIC-vertical and DIC-horizontal. Right column: AMO regressed onto d) DIC-vertical, e) DIC-horizontal, f) DIC-physical. Units mmol/ m³/yr.

Melissa 4/18/2016 7:17 PM

Deleted: 4

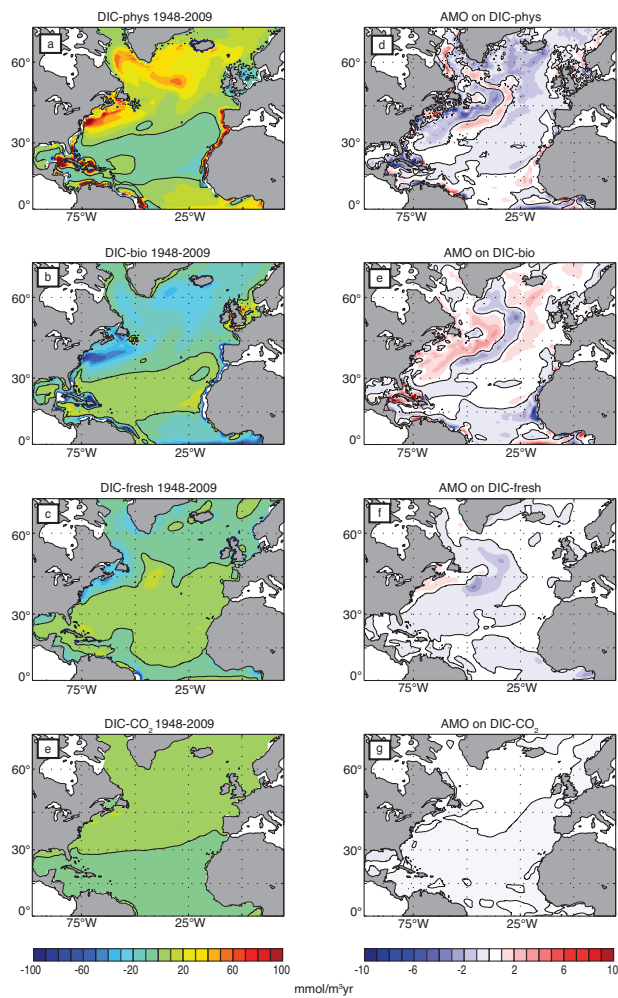


Figure 5: DIC diagnostics. Left column: 1948-2009 Mean a) DIC-physical, b) DIC-bio, c) DIC-fresh, d) DIC-CO₂flux . Right column: AMO regressed onto e) DIC-physical, f) DIC-bio , g) DIC-fresh, h) DIC-CO₂flux. Units mmol/m³/yr.

Melissa 4/18/2016 7:32 PM
Moved (insertion) [1]

Melissa 4/18/2016 7:32 PM
Moved (insertion) [2]

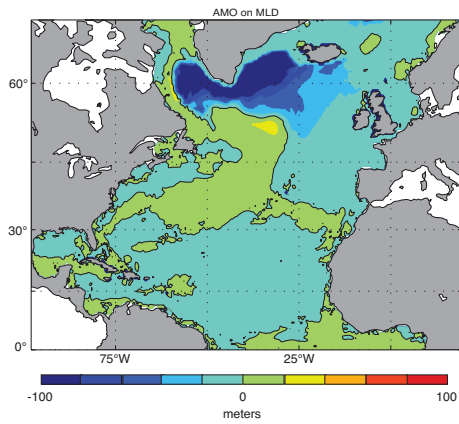


Figure 6: Regression of AMO on Mixed Layer Depth (MLD). Negative values denote a shoaling of MLD.

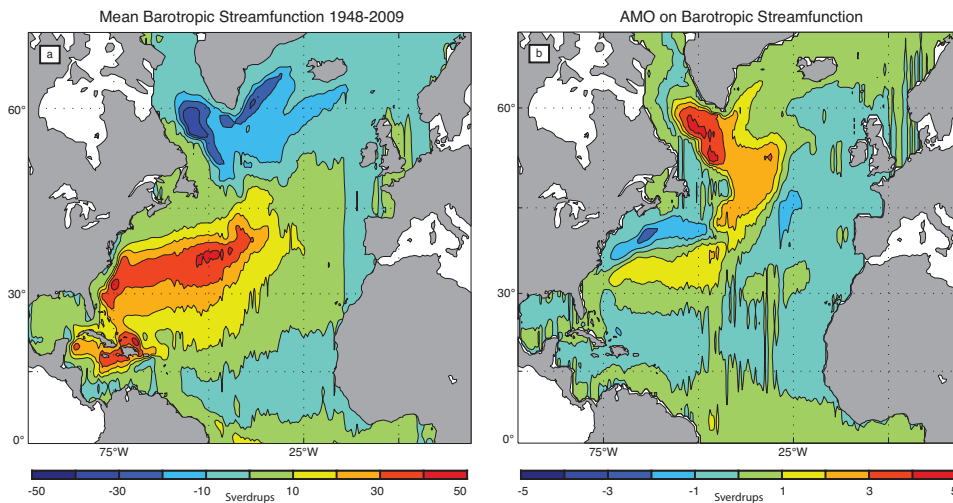


Figure 7: a) 1948-2009 mean barotropic streamfunction and b) AMO regressed onto barotropic streamfunction anomalies. Positive values denote clockwise motion. Units: Sverdrups ($1 \text{ Sv} = 10^6 \text{ m}^3 \text{ s}^{-1}$).

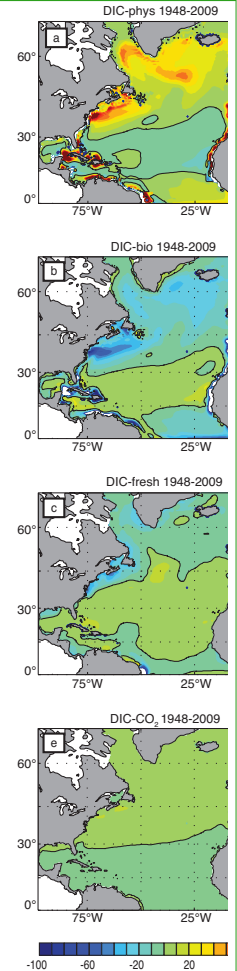
Melissa 4/18/2016 7:27 PM

Deleted: Figure 5: Regression of AMO on Mixed Layer Depth (MLD). Negative values denote a shoaling of MLD.

Melissa 4/18/2016 7:32 PM

Deleted: 6

Melissa 4/18/2016 7:32 PM



Moved up [1]:

Melissa 4/18/2016 7:32 PM

Moved up [2]: DIC diagnostics. Left column: 1948-2009 Mean a) DIC-physical, b) DIC-bio, c) DIC-fresh, d) DIC-CO₂flux. Right column: AMO regressed onto e) DIC-physical, f) DIC-bio, g) DIC-fresh, h) DIC-CO₂flux. Units mmol/m³/yr.

Melissa 4/18/2016 7:32 PM

Deleted:

... [1]

Supplementary Material for: Climate impacts on multidecadal pCO₂ variability in the North Atlantic: 1948-2009

Melissa L. Breeden and Galen A. McKinley

Supplementary Text:

To assess the model's ability to capture the vertical distribution of DIC, we compare here the 0-4000m average 1948-2009 model DIC profile to the GLODAP (Key et al. 2004) estimate of pre-industrial DIC across the subpolar gyre (35-55N, 5-60E, Figure S1). The model falls within the uncertainty of the observed estimate from 0-2000m, and is a few percent below the observed estimate from 2000-4000m. The average annual maximum MLD of this region is 284m and the annual maximum MLD across all points in the region is 3215m. Thus, annual vertical mixing occurs predominantly in the depth range where the model captures the observed estimate. In sum, this comparison suggests that model is a reasonable tool for studying how climate variability impacts variability in the vertical supply of carbon from the deep to surface ocean in the subpolar North Atlantic.

Melissa 4/18/2016 10:11 AM
Formatted: Font color: Auto

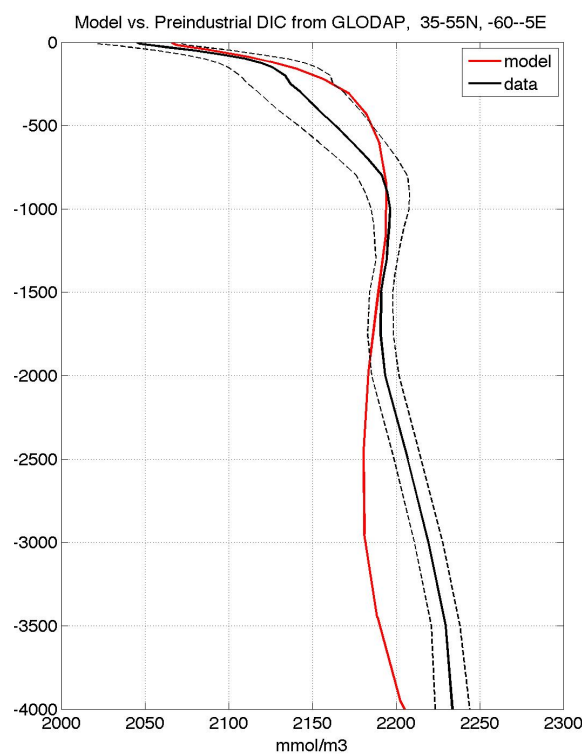


Figure S1: 35-55N, 5-60E average profile of 1948-2009 Model (red) and GLODAP preindustrial DIC (black) in mmol/m^3 .

Melissa 4/18/2016 10:11 AM
Formatted: Font color: Auto

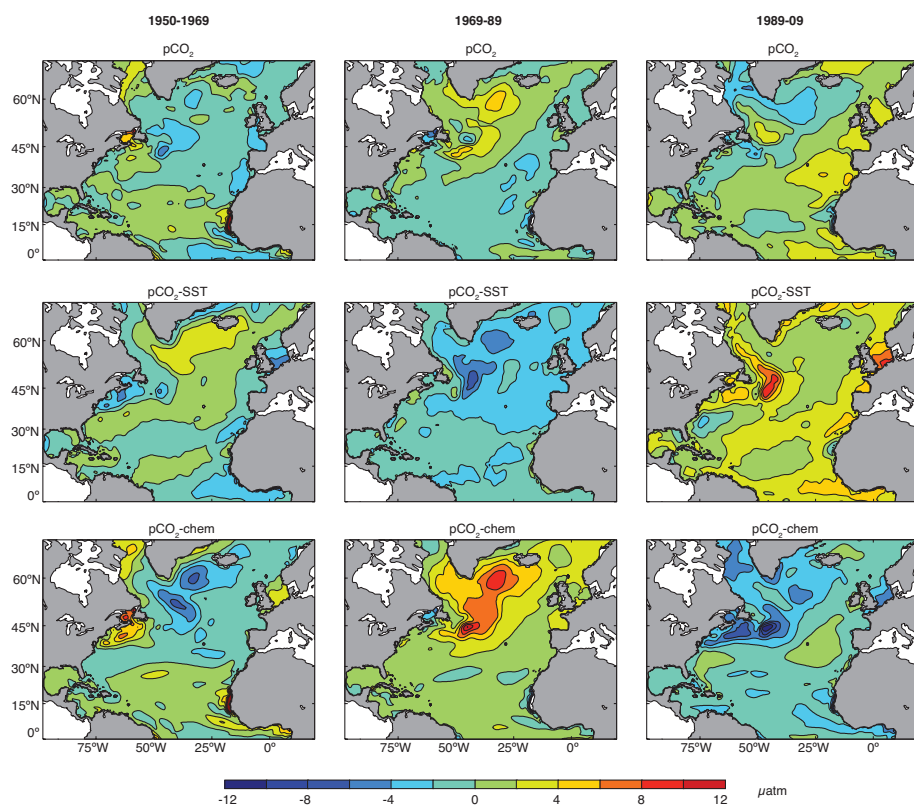


Figure S2: 20-year mean anomalies with respect to the 1948-2009 average for: a-c) $p\text{CO}_2$, d-f) $p\text{CO}_2\text{-SST}$, g-i) $p\text{CO}_2\text{-chem}$.

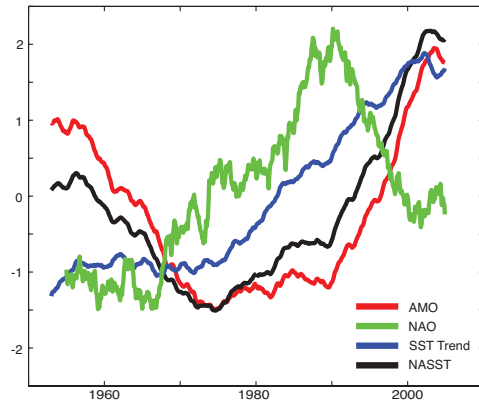


Figure S3: Same indices as in Figure 1d, as well as 121-month smoothed, standardized NAO index from NOAA ESRL (<http://www.esrl.noaa.gov/psd/data/climateindices/list/>).

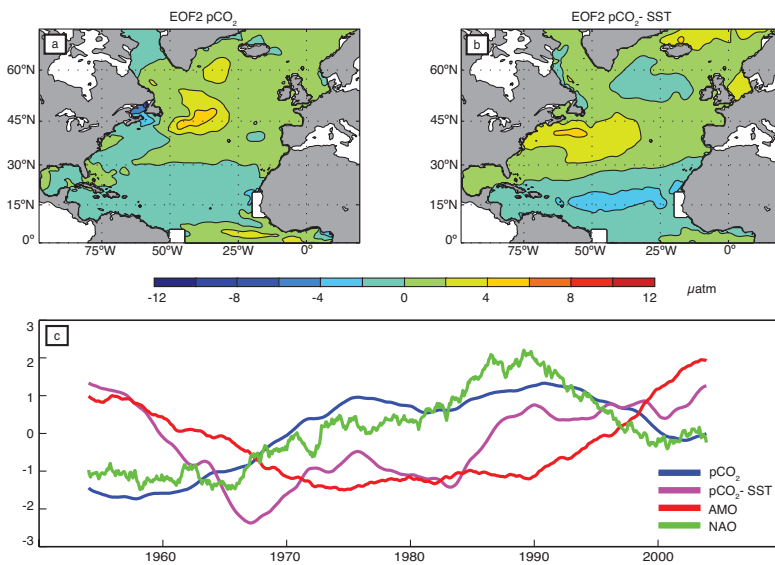


Figure S4: a) EOF2 of total $p\text{CO}_2$ (μatm), b) EOF2 of $p\text{CO}_2$ -SST (μatm), explaining 13% and 12% of total variance, respectively. c) PC2- $p\text{CO}_2$ (blue), PC2- $p\text{CO}_2$ -SST (pink), AMO index (red), and NAO index (green). Timeseries are smoothed with a 121-month box smoother.

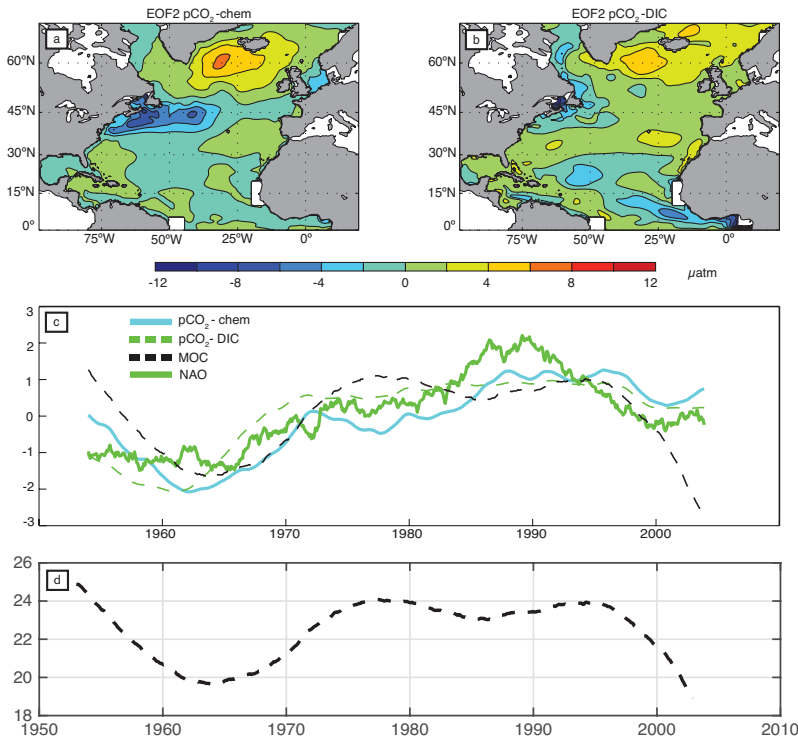
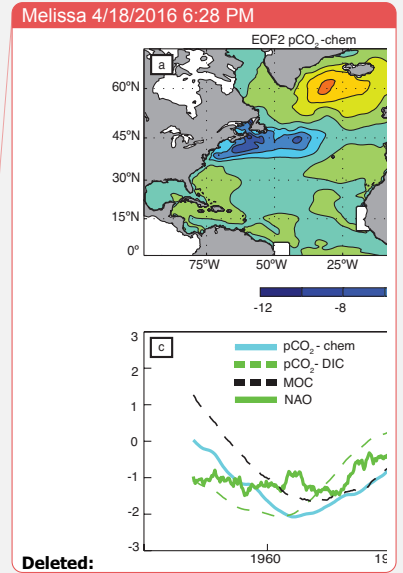


Figure S5: a) EOF2 pCO₂-chem (µatm), b) EOF2 pCO₂-DIC (µatm), each explaining 14% of total variance of each respective field. c) PC2- pCO₂-chem (cyan), PC2- pCO₂-DIC (green dash), NAO index (green), the modeled maximum Meridional Overturning Circulation at 45°N (MOC, black dash), all standardized. d) unstandardized MOC, units Sverdrups ($1SV = 10^6 \text{ m}^3 \text{ s}^{-1}$). Timeseries are smoothed with a 121-month box smoother.



Melissa 4/18/2016 6:15 PM
 Formatted: Superscript
 Melissa 4/18/2016 6:31 PM
 Formatted: Superscript
 Melissa 4/18/2016 6:31 PM
 Formatted: Superscript

	PC1- pCO ₂	PC1- pCO ₂ - SST	PC1- pCO ₂ - chem	PC1- pCO ₂ - DIC	PC1- pCO ₂ - ALK	SST	AMO	SST Trend	NAO	MOC
PC1- pCO ₂	1.0	0.91	0.66	0.67	-0.25	0.88	0.61	0.94	0.23	0.0026
PC1- pCO ₂ - SST		1.0	0.90	0.91	.05	1.0	0.86	0.78	- 0.069	-0.12
PC1- pCO ₂ - chem			1.0	0.98	.44	0.92	0.99	0.45	-0.42	-0.25
PC1- pCO ₂ - DIC				1.0	.35	0.93	0.96	0.49	-0.38	-0.18
PC1- pCO ₂ - ALK					1.0	.12	.48	-0.48	-0.70	-0.08
SST						1.0	0.90	0.74	-0.11	-0.13
AMO							1.0	0.37	-0.49	-0.32
SST Trend								1.0	0.51	0.21
NAO									1.0	0.57
MOC										1.0

Table S1: Correlation between first principle components of the EOFs for pCO₂ and its components, climate indices, and the modeled maximum Meridional Overturning Circulation (MOC) at 45°N. Index and MOC correlations are also shown. Bold indicates significance at the 95% level.

	PC2- pCO ₂ -	PC2- pCO ₂ - SST	PC2- pCO ₂ - chem	PC2- pCO ₂ - DIC	SST	AMO	SST Trend	NAO	MOC
PC2- pCO ₂ -	1.0	0.080	0.80	0.96	-0.18	-0.59	0.50	0.89	0.56
PC2- pCO ₂ - SST		1.0	0.52	-0.039	0.70	0.60	0.57	0.18	0.37
PC2- pCO ₂ - chem			1.0	0.82	0.28	-0.11	0.75	0.82	0.65
PC2- pCO ₂ - DIC				1.0	-0.12	-0.51	0.52	0.83	0.51

Table S2: Correlation between second principle components of the EOFs for pCO₂ and its components, climate indices, and MOC. Bold indicates significance at the 95% level.